Initial LCLS-II HXR Girder Positioning Calculation

Heinz-Dieter Nuhn[a]

[a]SLAC National Accelerator Laboratory, Stanford University, CA 94309-0210, USA

ABSTRACT

One of the more challenging tasks during the commissioning of the LCLS-II hard x-ray (HXR) undulator beamline is the initial electron transport through the very small aperture vacuum chamber without major beam losses. In order to achieve this, the initial positions of the quadrupoles (and thus the girders) need to be carefully chosen before the first beam transport is attempted. This document describes how the initial quadrupole positions are chosen such that the quadrupoles are positioned close to a straight line but with offsets that help compensate for any residual undulator and environmental magnetic fields.

Keywords: Undulator, Commissioning, LCLS-II, HXR, Alignment

1. INTRODUCTION

The initial transport through the narrow (5 mm × 11 mm) aperture and long (135 m-long) HXR undulator vacuum chamber is scheduled for June/July 2020. In order to minimize electron beam losses, and therefore high radiation doses, the initial position of the quadrupole magnets needs to be carefully considered. If the electron beam travels through a misaligned quadrupole it will receive a kick proportional to its offset to the quadrupole center, its energy and the quadrupole's gradient. The absolute value of the integrated quadrupole gradients will be set to 3 T, the sign of the gradient will alternate with every quadrupole to form a FODO lattice, with the first quadrupole in cell 13 being a horizontally focusing quadrupole, followed by a horizontally defocusing quadrupole in cell 14 etc.. Quadrupole focusing is important to prevent the electron beam from diverging and from getting lost in the vacuum chamber. Besides the kicks from misaligned quadrupoles, the beam will also receive kicks from environmental field components (EMF) (Earth Magnetic Field and local Undulator Hall magnetic fields, for instance from pump magnets etc.) as well as from undulator field integrals (small, unavoidable magnetic field compensation remnants). The goal is to compensate kicks from these extra fields by generating opposite sign kicks with the quadrupoles, which will be slightly misaligned for that purpose. The calculation of the initial quadrupole positions is based on a number of quantities that are described in the following section.

2. RELEVANT QUANTITIES

The initial transverse positions of the undulator line quadrupoles depends on the following quantities

- **Cam mover home positions:** For each HXR girder, five cam rollers can be used to move that girder in the transverse directions as well as change its roll pitch and yaw angles. Those movements are expressed relative to the cam rollers' home position. The home position for each cam roller is defined as the cam angle at which the girder contact surface is located half way between the two extreme vertical positions that it will assume when the angle goes through a full circle. The determination of the home position is done with the help of four linear potentiometers that are mounted close to the four corners of the girder to allow to measure the distance between the pedestals and the girder.
- **Metrological alignment girder positions:** Once, all components of the HXR undulator system are installed as they will be used during the initial commissioning phase, the SLAC Metrology group adjusts the cam roller support plates on top of the pedestals to bring the quadrupole axes close to a straight line between all installed quadrupoles. Before this alignment procedure, all cam rollers are set to their home positions (see above). After completing this procedure, the quadrupole centers deviate from a straight line by less than ±200 μm.

Further author information: E-mail: nuhn@slac.stanford.edu

- **Metrological quadrupole and undulator position mapping:** The final alignment step done by the Metrology group is the mapping of the locations of the quadrupole and undulator tooling balls. This information allows the calculation of the deviations of the magnetic axes of these components from a straight line. This task relies on the fact that the tooling balls on each quadrupole magnet and undulator segment have been fiducialized in the lab before the components got installed in the Undulator Hall (UH). Fiducialization is the procedure of measuring the coordinates of the tooling balls relative to a coordinate system that has its origin in the longitudinal center of the device on its magnetic axis.

- **Undulator segment field integrals with gaps open:** The undulator segments have very strong magnetic fields on axis that oscillate as function of z location (along the beam axis) within the devices. The undulator segments are designed so that their fields are compensated such that the average fields (averaged over a distance larger than the length of the device) are tiny compared to the absolute value of the peak field. But even these tiny field remnants are still large enough to be a significant source of phase errors if left uncompensated. Unfortunately, these residual amplitudes are dependent on the segment gap, i.e., they can not be fully compensated at all gaps. During the initial beam passage at the beginning of commissioning, the undulator segment gaps will be open, such that we are interested in the open gap values of the field integrals for this document.

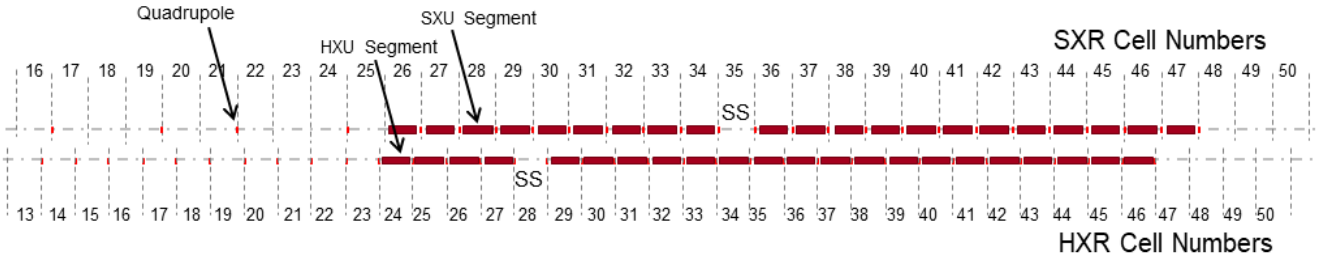

Figure 1: Schematic diagram of the layout of the undulator segment and quadrupole magnet arrangement during the initial LCLS-II HXR commissioning phase with the beam from the Cu linac in June or July 2020. The diagram also defines the cell numbers.

- **Environmental on-axis fields:** Before the undulator segments were installed in the UH, there was already a magnetic field component present, predominantly coming from the EMF with small contributions from local fields as they might be provided, for instance, by the permanent magnets in nearby vacuum pumps. The EMF is similar everywhere at SLAC but there are local changes of order 25%. The differences come from interactions with ferromagnetic components that are located in the vicinity of the locations were the measurements are performed. At the HXR bench in the SLAC Magnet Measurement Facility (MMF), the undulator segments have the same orientation relative to the EMF as they have when they are installed in the UH. Therefore, most of the effects of the EMF on the magnetic field on the axis of an undulator segment have been removed during the tuning process. Therefore, in the cells that have an undulator segment installed (see Fig. 1), only the difference between the local UH field and the MMF field needs to be compensated. This compensation is done with Environmental Field Correctors (EFCs), as described below. For cells without undulator segments, the full local environmental field needs compensation. The EMF amplitudes, measured on the virtual beam axis, are listed in appendix B.

- **EFC fields:** For the cells that have an undulator segment installed (see Fig. 1), we use four wires that are incorporated into the vacuum chamber to form EFCs These have been calibrated in the MMF and will automatically be set for the measured field differences between the MMF and the local fields. Because the local environmental field will be modified by the ferromagnetic components in the UH including the undulator segments, their effect on the beam, and thus the required EFC strength, depends on the undulator segment gap. The EFCs help to straighten the electron beam trajectory, which would otherwise have a small bow due to the field difference and would add significant phase delay to the electron beam. For those cells with installed undulator segments for which the EFC amplitude is set, the on-axis field is the same as in the MMF and no further environmental field correction is required.

- **Corrector fields:** In each cell is a horizontal and a vertical corrector integrated into the quadrupole magnet. Beam trajectory corrections can be done by either adjusting the current through the corrector coils or by changing the transverse position of the quadrupole magnet using the cam movers. For the initial setup as well for later Beam Based Alignment (BBA) procedures, the quadrupole position rather than the corrector amplitude will be used to straighten the beam trajectory. The correctors need to be set to zero current during these procedures. They will be used outside of these two procedures for temporary (up to the next BBA) trajectory corrections.
- **HXRSS chicane magnet fields:** The HXRSS chicane is made of four dipole magnets operated in series and a set of integrated trim coils. These magnets need to be deGaussed before the initial beam transport as well as during BBA.
- **Girder positioning:** Cam movers can be used to position the girders, which will move the quadrupoles. This mechanism will be used to straighten the beam trajectory during the initial setup and during BBA.

  Note: Cam mover controls uses a coordinate system that is centered in the quadrupole. Whenever this document talks about quadrupole cam alignment, quadrupole angle changes it will imply girder cam alignment and girder angle changes. This document does **not** talk about changing the quadruple position or angle alignments relative to the girder.

3. FORMULAE

The calculation of the initial quadrupole positions (cam angle settings) is based on four datasets:

- HXR Metrology Mapping Data (DX [mm], DY [mm], Yaw [mrad], Pitch [mrad]) provided by G. Gassner. (See Appendix A)
- HXR On-Axis EFM Data ($\langle B_x \rangle$ [T], $\langle B_y \rangle$ [T]) provided by S. Anderson. (See Appendix B)
- HXR Undulator Quadrupole Z Spacings (ΔZ [m]) according to the MAD deck and measured by the Metrology Group. (See Appendix C)
- HXR Undulator Segment Open Gap Field Integrals ($I1x$ [μTm], $I2x$ [μTm^2], $I1y$ [μTm], $I2y$ [μTm^2]) provided by Z. Wolf and Y. Levashov. (See Appendix D)

The following equations refer to the provided quantities through

(1)	Horizontal position misalignment of quadrupole in cell i:	"DX [mm]"/1000	$\Rightarrow$	$\Delta x_{Q,i}$
(2)	Vertical position misalignment of the ith quadrupole in cell i:	"DY [mm]"/1000	$\Rightarrow$	$\Delta y_{Q,i}$
(3)	Horizontal angle misalignment of the ith quadrupole in cell i:	"Yaw [mrad]"/1000	$\Rightarrow$	$\Delta \psi_{Q,i}$
(4)	Vertical angle misalignment of the ith quadrupole in cell i:	"Pitch [mrad]"/1000	$\Rightarrow$	$\Delta \theta_{Q,i}$
(5)	Average horizontal field between quadrupoles in cells $i-1$ and i:	"$\langle B_x \rangle$ [T]"	$\Rightarrow$	$\langle B_x \rangle_i$
(6)	Average vertical field between quadrupoles in cells $i-1$ and i:	"$\langle B_y \rangle$ [T]"	$\Rightarrow$	$\langle B_y \rangle_i$
(7)	Longitudinal distance between quadrupoles in cells $i-1$ and i:	"ΔZ [m]"	$\Rightarrow$	ΔL_i
(8)	First horizontal undulator field integral in cell i:	"$I1x$ [μTm]"/10^6	$\Rightarrow$	$I1x_i$
(9)	Second horizontal undulator field integral in cell i:	"$I2x$ [μTm]"/10^6	$\Rightarrow$	$I2x_i$
(10)	First vertical undulator field integral in cell i:	"$I1y$ [μTm]"/10^6	$\Rightarrow$	$I1y_i$
(11)	Second vertical undulator field integral in cell i:	"$I2y$ [μTm]"/10^6	$\Rightarrow$	$I2y_i$

Note: For items (5) and (6), the fields for the first cell (13) start from an equivalent upstream quadrupole position, since there is no physical quadrupole directly upstream of that cell. See Fig. 1 for cell definitions and section 3.6 for further explanation.

The corrective quadrupole movement needs to cover two components: residual misalignments (corrections $\Delta x_{\mathrm{M}et,i}$, $\Delta y_{\mathrm{M}et,i}$, $\Delta \psi_{\mathrm{M}et,i}$ and $\Delta \theta_{\mathrm{M}et,i}$), as well a the compensation of residual magnetic fields (corrections $\Delta x_{\mathrm{B},i}$ and $\Delta y_{\mathrm{B},i}$). For the latter a corresponding adjustment for the yaw and pitch angles will also be necessary in order to keep the transverse proximity between the upstream end of the adjusted girder and the upstream quadrupole (corrections $\Delta \psi_{\mathrm{B},i}$, and $\Delta \theta_{\mathrm{B},i}$)

3.1. CORRECTION OF QUADRUPOLE MISALIGNMENTS

The corrections of the residual misalignments are done by moving the quadrupoles in the opposite direction to the position in which they were measured, i.e.,

$$\Delta x_{\mathrm{Met},i} = -\Delta x_{\mathrm{Q},i} \tag{1}$$

$$\Delta y_{\mathrm{Met},i} = -\Delta y_{\mathrm{Q},i} \tag{2}$$

$$\Delta \psi_{\mathrm{Met},i} = -\Delta \psi_{\mathrm{Q},i} \tag{3}$$

$$\Delta \theta_{\mathrm{Met},i} = -\Delta \theta_{\mathrm{Q},i} \tag{4}$$

3.2. MOVING QUADRUPOLES TO GENERATE KICKS TO THE ELECTRON BEAM

In a quadrupole magnet, the components of the magnetic field change linearly with distance, Δx, Δy, from the center.

$$B_x = \frac{\partial B_x}{\partial y}\Delta y \tag{5}$$

$$B_y = \frac{\partial B_y}{\partial x}\Delta x. \tag{6}$$

In a quadrupole magnet, the horizontal and vertical gradients are identical. We will replace them with the symbol $-G$, for gradient, i.e.

$$G = -\frac{\partial B_x}{\partial y} = -\frac{\partial B_y}{\partial x}. \tag{7}$$

The Lorentz force equation tells us that the force that acts on the beam as it enters the quadrupole with speed close to the speed of light, c, i.e., $v_z \approx c$, is

$$\overrightarrow{F} = -e\overrightarrow{v} \times \overrightarrow{B} \approx -e\left(0,0,c\right) \times \left(B_x, B_y, 0\right) = ec\left(B_y, -B_x, 0\right). \tag{8}$$

The "$-$" sign in the second term indicates that we are working with electrons, which have a negative charge.

The magnetic field vanishes in the center of the quadrupole magnet. The beam will not be bent when it enters the quadrupole in its center. If the quadrupole is moved in horizontal direction by an amount Δx_Q, the beam will be moved off the center of the quadrupole in the opposite direction by $-\Delta x_Q$ and will experience the horizontal force

$$F_x\left(z\right) = ec\frac{\partial B_y\left(z\right)}{\partial x}\left(-\Delta x_Q\right) = -ec\frac{\partial B_y\left(z\right)}{\partial x}\Delta x_Q = +ecG\left(z\right)\Delta x_Q, \tag{9}$$

If G is positive, i.e. $\partial B_y/\partial x$ is negative, the force will be directed towards the quadrupole center, i.e, the quadrupole is horizontally focusing.

On the other hand, if the quadrupole is moved in y direction by an amount Δy_Q, the beam will be moved off the center of the quadrupole in the opposite direction by $-\Delta y_Q$ and will experience the force

$$F_y\left(z\right) = -ec\frac{\partial B_x\left(z\right)}{\partial y}\left(-\Delta y_Q\right) = +ec\frac{\partial B_x\left(z\right)}{\partial y}\Delta y_Q = -ecG\left(z\right)\Delta y_Q, \tag{10}$$

Here, if G is positive, i.e. $\partial B_x/\partial y$ is negative, the force will be directed away from the quadrupole center, i.e, the quadrupole is vertically defocusing.

The total kick amplitudes, $\Delta x'$ and $\Delta y'$ is given by

$$\Delta x' = \frac{1}{c}\int_{-\infty}^{+\infty}\frac{1}{\gamma m_e}F_x\left(\tilde{z}\right)dt = \frac{1}{\gamma m_e c^2}\int_{-\infty}^{+\infty}F_x\left(\tilde{z}\right)d\tilde{z} = \frac{ec}{\gamma m_e c^2}\Delta x_Q\int_{-\infty}^{+\infty}G\left(\tilde{z}\right)d\tilde{z} = \frac{(IG)}{B\rho}\Delta x_Q \tag{11}$$

$$\Delta y' = \frac{1}{c}\int_{-\infty}^{+\infty}\frac{1}{\gamma m_e}F_y\left(\tilde{z}\right)dt = \frac{1}{\gamma m_e c^2}\int_{-\infty}^{+\infty}F_y\left(\tilde{z}\right)d\tilde{z} = -\frac{ec}{\gamma m_e c^2}\Delta y_Q\int_{-\infty}^{+\infty}G\left(\tilde{z}\right)d\tilde{z} = -\frac{(IG)}{B\rho}\Delta y_Q \tag{12}$$

The term $B\rho = p/e \approx E/(ec) = \gamma m_e c^2/(ec)$, about 45.5 Tm for an energy of $E \approx 13.64$ GeV, is the magnetic rigidity, with momentum, p, speed of light, c, and electron charge, e. The integral has been abbreviated by the symbol (IG), which is the integrated gradient of the quadrupole magnet measured in units of [T].

The quadrupole moves, required to generate certain kick angles $\Delta x'$, $\Delta y'$, are then

$$\Delta x_Q = +\frac{B\rho}{(IG)}\Delta x' \tag{13}$$

$$\Delta y_Q = -\frac{B\rho}{(IG)}\Delta y' \tag{14}$$

3.3. CORRECTION OF RESIDUAL MAGNETIC FIELDS

The effect of the residual magnetic field in cell, i, can be expressed as a transverse kick in each plane (horizontal and vertical) centered between two adjacent quadrupoles, $i-1$ and i, spaced by distance ΔL_i:

$$\Delta x'_{env,i} = +\frac{\langle B_y\rangle_i \Delta L_i}{B\rho} \tag{15}$$

$$\Delta y'_{env,i} = -\frac{\langle B_x\rangle_i \Delta L_i}{B\rho}. \tag{16}$$

The overall effect of this kick can be minimized (localized) by converting it into a closed bump, using the quadrupole upstream and the quadrupole downstream as additional kickers. The kick angle required from either quadrupole is the same, i.e., $-\Delta x'_{env,i}/2$ and $-\Delta y'_{env,i}/2$ for the horizontal and vertical plane, respectively.

Note: $\Delta x'_{env,i}$ and $\Delta y'_{env,i}$ should be set to 0 if an undulator segment is installed in cell i.

The required moves of the upstream quadrupole, $i-1$, for the correction of a residual magnetic field in cell i are

$$\Delta x_{B,\mathrm{us},env,i-1} = -\frac{\Delta x'_{env,i}}{2}\left(+\frac{B\rho}{(IG)_{i-1}}\right) = -\frac{1}{2}\left(+\frac{\langle B_y\rangle_i \Delta L_i}{B\rho}\right)\left(+\frac{B\rho}{(IG)_{i-1}}\right) = -\frac{1}{2}\frac{\langle B_y\rangle_i \Delta L_i}{(IG)_{i-1}} \tag{17}$$

$$\Delta y_{B,\mathrm{us},env,i-1} = -\frac{\Delta y'_{env,i}}{2}\left(-\frac{B\rho}{(IG)_{i-1}}\right) = -\frac{1}{2}\left(-\frac{\langle B_x\rangle_i \Delta L_i}{B\rho}\right)\left(-\frac{B\rho}{(IG)_{i-1}}\right) = -\frac{1}{2}\frac{\langle B_x\rangle_i \Delta L_i}{(IG)_{i-1}}. \tag{18}$$

The required moves by the downstream quadrupole, i, for the correction of a residual magnetic field in cell i are

$$\Delta x_{B,\mathrm{ds},env,i} = -\frac{\Delta x'_{env,i}}{2}\left(+\frac{B\rho}{(IG)_i}\right) = -\frac{1}{2}\left(+\frac{\langle B_y\rangle_i \Delta L_i}{B\rho}\right)\left(+\frac{B\rho}{(IG)_i}\right) = -\frac{1}{2}\frac{\langle B_y\rangle_i \Delta L_i}{(IG)_i} \tag{19}$$

$$\Delta y_{B,\mathrm{ds},env,i} = -\frac{\Delta y'_{env,i}}{2}\left(-\frac{B\rho}{(IG)_i}\right) = -\frac{1}{2}\left(-\frac{\langle B_x\rangle_i \Delta L_i}{B\rho}\right)\left(-\frac{B\rho}{(IG)_i}\right) = -\frac{1}{2}\frac{\langle B_x\rangle_i \Delta L_i}{(IG)_i}. \tag{20}$$

Moves of quadrupole i, necessary to make partial corrections for both adjacent cells, i and $i+1$, are

$$\Delta x_{B,env,i} = \Delta x_{B,\mathrm{us},env,i} + \Delta x_{B,\mathrm{ds},env,i} = -\frac{1}{2\,(IG)_i}\left(\langle B_y\rangle_{i+1}\Delta L_{i+1} + \langle B_y\rangle_i \Delta L_i\right) \tag{21}$$

$$\Delta y_{B,env,i} = \Delta y_{B,\mathrm{us},env,i} + \Delta y_{B,\mathrm{ds},env,i} = -\frac{1}{2\,(IG)_i}\left(\langle B_x\rangle_{i+1}\Delta L_{i+1} + \langle B_x\rangle_i \Delta L_i\right), \tag{22}$$

using the integrated gradient, $(IG)_i$, of the quadrupole in cell i, which is +3 T for horizontally focusing quadrupoles and −3 T for horizontally defocusing quadrupoles. The two terms in Eqs. 21 and 22 take into account that each quadrupole has to fulfill two functions: terminating the bump from the previous drift section and starting a new bump for the following drift section. The first and last quadrupole in the line only need to use one of these terms.

The yaw and pitch corrections of the girder in cell i are done such that the girder in cell i is pivoted with respect to the center of quadrupole in cell i such that the upstream end of the girder follows the move of the quadrupole on the girder in cell $i-1$:

$$\Delta\psi_{B,env,i} = \arctan\left(\frac{\Delta x_{B,env,i} - \Delta x_{B,env,i-1}}{\Delta L_i}\right) \approx \frac{\Delta x_{B,env,i} - \Delta x_{B,env,i-1}}{\Delta L_i} = \\ = -\frac{1}{\Delta L_i}\left(\frac{\langle B_y\rangle_{i+1}\Delta L_{i+1} + \langle B_y\rangle_i \Delta L_i)}{2\,(IG)_i} - \frac{\langle B_y\rangle_i \Delta L_i + \langle B_y\rangle_{i-1}\Delta L_{i-1}}{2\,(IG)_{i-1}}\right) \quad (23)$$

$$\Delta\theta_{B,env,i} = \arctan\left(\frac{\Delta y_{B,env,i} - \Delta y_{B,env,i-1}}{\Delta L_i}\right) \approx \frac{\Delta y_{B,env,i} - \Delta y_{B,env,i-1}}{\Delta L_i} = \\ = -\frac{1}{\Delta L_i}\left(\frac{\langle B_x\rangle_{i+1}\Delta L_{i+1} + \langle B_x\rangle_i \Delta L_i}{2\,(IG)_i} - \frac{\langle B_x\rangle_i \Delta L_i + \langle B_x\rangle_{i-1}\Delta L_{i-1}}{2\,(IG)_{i-1}}\right) \quad (24)$$

3.4. CORRECTION OF UNDULATOR FIELD INTEGRALS

The undulator field integrals cause an electron beam, that enters an undulator on-axis, to exit that undulator with offsets $\Delta x_{\mathrm{int},i}$ and $\Delta y_{\mathrm{int},i}$ as well as slopes $\Delta x'_{\mathrm{int},i}$ and $\Delta y'_{\mathrm{int},i}$:

$$\Delta x_{\mathrm{int},i} = \frac{I2y_i}{B\rho} \quad (25)$$

$$\Delta x'_{\mathrm{int},i} = \frac{I1y_i}{B\rho} \quad (26)$$

$$\Delta y_{int,i} = -\frac{I2x_i}{B\rho} \quad (27)$$

$$\Delta y'_{int,i} = -\frac{I1x_i}{B\rho}. \quad (28)$$

This trajectory disturbance can be converted into a localized bump by kicking the beam with the upstream, cell $i-1$, and downstream, cell i, quadrupoles. The required corrective kick amplitudes are

$$\Delta x'_{int,entr-cor,i-1} = -\frac{\Delta x_{\mathrm{int},i}}{\Delta L_i} = -\frac{I2y_i}{B\rho\Delta L_i} \quad (29)$$

$$\Delta x'_{int,exit-cor,i} = -\Delta x'_{\mathrm{int},i} + \frac{\Delta x_{\mathrm{int},i}}{\Delta L_i} = -\frac{I1y_i}{B\rho} + \frac{I2y_i}{B\rho\Delta L_i} \quad (30)$$

$$\Delta y'_{int,entr-cor,i-1} = -\frac{\Delta y_{\mathrm{int},i}}{\Delta L_i} = \frac{I2x_i}{B\rho\Delta L_i} \quad (31)$$

$$\Delta y'_{int,exit-cor,i} = -\Delta y'_{\mathrm{int},i} + \frac{\Delta y_{\mathrm{int},i}}{\Delta L_i} = \frac{I1x_i}{B\rho} - \frac{I2x_i}{B\rho\Delta L_i}. \quad (32)$$

The move of the quadrupole in cell i (see Fig. 1), necessary to achieve these kicks, are

$$\Delta x_{B,int,i} = +\left(\Delta x'_{int,exit-cor,i} + \Delta x'_{int,entr-cor,i}\right)\frac{B\rho}{(IG)_i} = +\left(-I1y_i + \frac{I2y_i}{\Delta L_i} - \frac{I2y_{i+1}}{\Delta L_{i+1}}\right)\frac{1}{(IG)_i} = \\ = -\left(I1y_i - \frac{I2y_i}{\Delta L_i} + \frac{I2y_{i+1}}{\Delta L_{i+1}}\right)\frac{1}{(IG)_i} \quad (33)$$

$$\Delta y_{B,int,i} = -\left(\Delta y'_{int,exit-cor,i} + \Delta y'_{int,entr-cor,i}\right)\frac{B\rho}{(IG)_i} = \\ = -\left(I1x_i - \frac{I2x_i}{\Delta L_i} + \frac{I2x_{i+1}}{\Delta L_{i+1}}\right)\frac{1}{(IG)_i}. \quad (34)$$

Note: the required corrections are independent of electron beam energy because they are either positional corrections or field compensations.

The yaw and pitch corrections of the girder in cell i are done such that the girder in cell i is pivoted with respect to the center of quadrupole in cell i such that the upstream end of the girder follows the move of the quadrupole on the girder in cell $i-1$:

$$\Delta\psi_{B,int,i} = \arctan\left(\frac{\Delta x_{B,int,i} - \Delta x_{B,int,i-1}}{\Delta L_i}\right) = \frac{\Delta x_{B,int,i} - \Delta x_{B,int,i-1}}{\Delta L_i} = \\ = -\frac{1}{\Delta L_i}\left(\frac{1}{(IG)_i}\left(I1y_i - \frac{I2y_i}{\Delta L_i} + \frac{I2y_{i+1}}{\Delta L_{i+1}}\right) - \frac{1}{(IG)_{i-1}}\left(I1y_{i-1} - \frac{I2y_{i-1}}{\Delta L_{i-1}} + \frac{I2y_i}{\Delta L_i}\right)\right) \quad (35)$$

$$\Delta\theta_{B,int,i} = \arctan\left(\frac{\Delta y_{B,int,i} - \Delta y_{B,int,i-1}}{\Delta L_i}\right) = \frac{\Delta y_{B,int,i} - \Delta y_{B,int,i-1}}{\Delta L_i} = \\ = -\frac{1}{\Delta L_i}\left(\frac{1}{(IG)_i}\left(I1x_i - \frac{I2x_i}{\Delta L_i} + \frac{I2x_{i+1}}{\Delta L_{i+1}}\right) - \frac{1}{(IG)_{i-1}}\left(I1x_{i-1} - \frac{I2x_{i-1}}{\Delta L_{i-1}} + \frac{I2x_i}{\Delta L_i}\right)\right). \quad (36)$$

3.5. TOTAL REQUIRED QUADRUPOLE MOVES FOR HXR CELLS 24 TO 27 AND 29 TO 45

This section is for those 21 cells that have an undulator segment installed, but are not end cells. The total quadrupole moves required to compensate for both the undulator field integral and the environmental fields are

$$\Delta x_i = \Delta x_{\mathrm{Met},i} + \Delta x_{B,env,i} + \Delta x_{B,int,i} \quad (37)$$

$$\Delta y_i = \Delta y_{\mathrm{Met},i} + \Delta y_{B,env,i} + \Delta y_{B,int,i} \quad (38)$$

$$\Delta\psi_i = \Delta\psi_{\mathrm{Met},i} + \Delta\psi_{B,env,i} + \Delta\psi_{B,int,i} \quad (39)$$

$$\Delta\theta_i = \Delta\theta_{\mathrm{Met},i} + \Delta\theta_{B,env,i} + \Delta\theta_{B,int,i} \quad (40)$$

After inserting the terms that we derived, above, we get

$$\Delta x_i = -\Delta x_{\mathrm{Q},i} - \frac{1}{2\,(IG)_i}\left(\langle B_y\rangle_{i+1}\,\Delta L_{i+1} + \langle B_y\rangle_i\,\Delta L_i\right) - \frac{1}{(IG)_i}\left(I1y_i - \frac{I2y_i}{\Delta L_i} + \frac{I2y_{i+1}}{\Delta L_{i+1}}\right) \quad (41)$$

$$\Delta y_i = -\Delta y_{\mathrm{Q},i} - \frac{1}{2\,(IG)_i}\left(\langle B_x\rangle_{i+1}\,\Delta L_{i+1} + \langle B_x\rangle_i\,\Delta L_i\right) - \frac{1}{(IG)_i}\left(I1x_i - \frac{I2x_i}{\Delta L_i} + \frac{I2x_{i+1}}{\Delta L_{i+1}}\right) \quad (42)$$

$$\Delta\psi_i = -\Delta\psi_{\mathrm{Q},i} + \frac{\Delta x_{B,env,i} - \Delta x_{B,env,i-1}}{\Delta L_i} + \frac{\Delta x_{B,int,i} - \Delta x_{B,int,i-1}}{\Delta L_i} \quad (43)$$

$$\Delta\theta_i = -\Delta\theta_{\mathrm{Q},i} + \frac{\Delta y_{B,env,i} - \Delta y_{B,env,i-1}}{\Delta L_i} + \frac{\Delta y_{B,int,i} - \Delta y_{B,int,i-1}}{\Delta L_i} \quad (44)$$

$$\Delta\psi_i = -\Delta\psi_{\mathrm{Q},i} - \frac{1}{\Delta L_i}\left(\frac{\left(\langle B_y\rangle_{i+1}\,\Delta L_{i+1} + \langle B_y\rangle_i\,\Delta L_i\right)}{2\,(IG)_i} - \frac{\left(\langle B_y\rangle_i\,\Delta L_i + \langle B_y\rangle_{i-1}\,\Delta L_{i-1}\right)}{2\,(IG)_{i-1}}\right) - \\ - \frac{1}{\Delta L_i}\left(\frac{1}{(IG)_i}\left(I1y_i - \frac{I2y_i}{\Delta L_i} + \frac{I2y_{i+1}}{\Delta L_{i+1}}\right) - \frac{1}{(IG)_{i-1}}\left(I1y_{i-1} - \frac{I2y_{i-1}}{\Delta L_{i-1}} + \frac{I2y_i}{\Delta L_i}\right)\right) \quad (45)$$

$$\Delta\theta_i = -\Delta\theta_{\mathrm{Q},i} - \frac{1}{\Delta L_i}\left(\frac{\left(\langle B_x\rangle_{i+1}\,\Delta L_{i+1} + \langle B_x\rangle_i\,\Delta L_i\right)}{2\,(IG)_i} - \frac{\left(\langle B_x\rangle_i\,\Delta L_i + \langle B_x\rangle_{i-1}\,\Delta L_{i-1}\right)}{2\,(IG)_{i-1}}\right) - \\ - \frac{1}{\Delta L_i}\left(\frac{1}{(IG)_i}\left(I1x_i - \frac{I2x_i}{\Delta L_i} + \frac{I2x_{i+1}}{\Delta L_{i+1}}\right) - \frac{1}{(IG)_{i-1}}\left(I1x_{i-1} - \frac{I2x_{i-1}}{\Delta L_{i-1}} + \frac{I2x_i}{\Delta L_i}\right)\right) \quad (46)$$

3.6. TOTAL REQUIRED QUADRUPOLE MOVES FOR HXR CELL13

For the first HXR girder the equations are

$$\Delta x_{B,env,13} = -\Delta x_{\mathrm{Q},13} - \frac{1}{(IG)_{13}} \left(\frac{1}{2} \langle B_y \rangle_{14} \Delta L_{14} + \langle B_y \rangle_{13} \Delta L_{16} \right) \tag{47}$$

$$\Delta y_{B,env,13} = -\Delta y_{\mathrm{Q},13} - \frac{1}{(IG)_{13}} \left(\frac{1}{2} \langle B_x \rangle_{14} \Delta L_{14} + \langle B_x \rangle_{13} \Delta L_{16} \right). \tag{48}$$

$$\Delta \psi_{B,env,13} = -\Delta \psi_{\mathrm{Q},13} - \frac{1}{\Delta L_{16}} \frac{1}{(IG)_{13}} \left(\frac{1}{2} \langle B_y \rangle_{14} \Delta L_{14} + \langle B_y \rangle_{13} \Delta L_{16} \right) \tag{49}$$

$$\Delta \theta_{B,env,13} = -\Delta \theta_{\mathrm{Q},13} - \frac{1}{\Delta L_{16}} \frac{1}{(IG)_{13}} \left(\frac{1}{2} \langle B_x \rangle_{14} \Delta L_{14} + \langle B_x \rangle_{13} \Delta L_{16} \right). \tag{50}$$

Because there is no undulator segment installed on girder 13, no undulator field integrals need to be compensated.

We are using ΔL_{16} here because there is no quadrupole in front of cell 13 and therefore ΔL_{13} can not be determined by the formula given above. At the beginning of the HXR line, there are still the old girders installed, which have a ''short-short-long" quadrupole spacing pattern, which makes cell 16 equivalent to cell 13.

This form of the equation leaves a small offset after cell 13. Because there is no corrector right in front of girder 13, only the angle errors, not the offset errors from error fields on girder 13 will be corrected.

3.7. TOTAL REQUIRED QUADRUPOLE MOVES FOR HXR CELLS 14 TO 23 AND 28

This section is for those 11 cells that don't have an undulator segment installed and are not end cells. For those cells only the compensation of the environmental field is needed. The required quadrupole move are

$$\Delta x_i = \Delta x_{\mathrm{Met},i} + \Delta x_{B,env,i} \tag{51}$$

$$\Delta y_i = \Delta y_{\mathrm{Met},i} + \Delta y_{B,env,i} \tag{52}$$

$$\Delta \psi_i = \Delta \psi_{\mathrm{Met},i} + \Delta \psi_{B,env,i} \tag{53}$$

$$\Delta \theta_i = \Delta \theta_{\mathrm{Met},i} + \Delta \theta_{B,env,i} \tag{54}$$

After inserting the terms that we derived, above, we get

$$\Delta x_i = -\Delta x_{\mathrm{Q},i} - \frac{1}{2\,(IG)_i} \left(\langle B_y \rangle_{i+1} \Delta L_{i+1} + \langle B_y \rangle_i \Delta L_i \right) \tag{55}$$

$$\Delta y_i = -\Delta y_{\mathrm{Q},i} - \frac{1}{2\,(IG)_i} \left(\langle B_x \rangle_{i+1} \Delta L_{i+1} + \langle B_x \rangle_i \Delta L_i \right) \tag{56}$$

$$\Delta \psi_i = -\Delta \psi_{\mathrm{Q},i} - \frac{1}{\Delta L_i} \left(\frac{\langle B_y \rangle_{i+1} \Delta L_{i+1} - \langle B_y \rangle_i \Delta L_i}{2\,(IG)_i} - \frac{\langle B_y \rangle_i \Delta L_i + \langle B_y \rangle_{i-1} \Delta L_{i-1}}{2\,(IG)_{i-1}} \right) \tag{57}$$

$$\Delta \theta_i = -\Delta \theta_{\mathrm{Q},i} - \frac{1}{\Delta L_i} \left(\frac{\langle B_x \rangle_{i+1} \Delta L_{i+1} + \langle B_x \rangle_i \Delta L_i}{2\,(IG)_i} - \frac{\langle B_x \rangle_i \Delta L_i + \langle B_x \rangle_{i-1} \Delta L_{i-1}}{2\,(IG)_{i-1}} \right). \tag{58}$$

3.8. TOTAL REQUIRED QUADRUPOLE MOVES FOR HXR CELL 46

For the last HXR girder, the equations are

$$\Delta x_{46} = -\Delta x_{\mathrm{Q},46} - \frac{1}{2\left(IG\right)_{46}}\left(\left\langle B_y\right\rangle_{46}\Delta L_{46}\right) - \frac{1}{\left(IG\right)_{46}}\left(I1y_{46} - \frac{I2y_{46}}{\Delta L_{46}}\right) \tag{59}$$

$$\Delta y_{46} = -\Delta y_{\mathrm{Q},46} - \frac{1}{2\left(IG\right)_{46}}\left(\left\langle B_x\right\rangle_{46}\Delta L_{46}\right) - \frac{1}{\left(IG\right)_{46}}\left(I1x_{46} - \frac{I2x_{46}}{\Delta L_{46}}\right) \tag{60}$$

$$\begin{aligned}\Delta\psi_{46} = -\Delta\psi_{\mathrm{Q},46} - \frac{1}{\Delta L_{46}}\left(\frac{\left\langle B_y\right\rangle_{46}\Delta L_{46}}{2\left(IG\right)_{46}} - \frac{\left\langle B_y\right\rangle_{46}\Delta L_{46} + \left\langle B_y\right\rangle_{45}\Delta L_{45}}{2\left(IG\right)_{45}}\right) - \\ - \frac{1}{\Delta L_{46}}\left(\frac{1}{\left(IG\right)_{46}}\left(I1y_{46} - \frac{I2y_{46}}{\Delta L_{46}}\right) - \frac{1}{\left(IG\right)_{45}}\left(I1y_{45} - \frac{I2y_{45}}{\Delta L_{45}} + \frac{I2y_{46}}{\Delta L_{46}}\right)\right)\end{aligned} \tag{61}$$

$$\begin{aligned}\Delta\theta_{46} = -\Delta\theta_{\mathrm{Q},46} - \frac{1}{\Delta L_{46}}\left(\frac{\left\langle B_x\right\rangle_{46}\Delta L_{46}}{2\left(IG\right)_{46}} - \frac{\left\langle B_x\right\rangle_{46}\Delta L_{46} + \left\langle B_x\right\rangle_{45}\Delta L_{45}}{2\left(IG\right)_{45}}\right) - \\ - \frac{1}{\Delta L_{46}}\left(\frac{1}{\left(IG\right)_{46}}\left(I1x_{46} - \frac{I2x_{46}}{\Delta L_{46}}\right) - \frac{1}{\left(IG\right)_{45}}\left(I1x_{45} - \frac{I2x_{45}}{\Delta L_{45}} + \frac{I2x_{46}}{\Delta L_{46}}\right)\right)\end{aligned} \tag{62}$$

Table 1: Required quadrupole moves relative to the cam home positions for the first beam through the HXR beam pipe during Cu-linac commissioning taking all contributions into account.

Cell	Δx [μm]	Δy [μm]	$\Delta\psi$ [μrad]	$\Delta\theta$ [μrad]
13	−88.4	−76.3	+21.90	−0.91
14	−153.7	−116.3	−39.55	+1.26
15	+116.5	+31.4	+33.47	−1.72
16	−151.5	+7.8	−34.56	+2.56
17	−11.8	−155.5	+34.66	−4.37
18	−81.3	−176.5	−31.44	+5.12
19	−36.5	−41.1	+32.78	−4.06
20	−86.9	−41.2	−42.22	+1.48
21	−58.0	+47.0	+42.12	−1.08
22	−172.0	+31.0	−38.03	+3.34
23	−37.1	+88.4	+37.52	−6.97
24	−233.3	−122.4	−66.95	−18.23
25	−82.0	−81.0	+36.79	+3.39
26	−219.9	−99.4	−32.44	+12.34
27	−128.7	−178.4	+27.41	−21.90
28	−227.8	−1.3	−32.43	+9.43
29	−88.4	−84.1	+27.84	+18.55
30	−251.3	−79.3	−57.48	+0.12
31	−120.1	−54.8	+20.05	−7.52
32	−199.0	+37.4	−32.46	+55.09
33	−94.2	−108.5	+7.59	+18.92
34	−128.6	−54.7	−52.71	+15.66
35	+55.2	−289.6	+58.93	−42.25
36	−85.6	−2.5	−41.51	+4.10
37	−141.1	−66.3	−8.87	−20.32
38	−279.7	+174.2	−108.92	+18.82
39	+49.2	−50.0	−12.52	−9.81
40	+19.7	−115.4	+22.36	−34.90
41	+68.9	+15.3	+19.42	−14.39
42	−97.7	+78.2	−21.69	+44.03
43	+59.0	+73.8	+0.81	+35.24
44	+58.2	−42.2	−56.09	+3.80
45	+61.8	−164.1	−15.36	−18.40
46	+51.7	+2.1	−18.30	+4.12

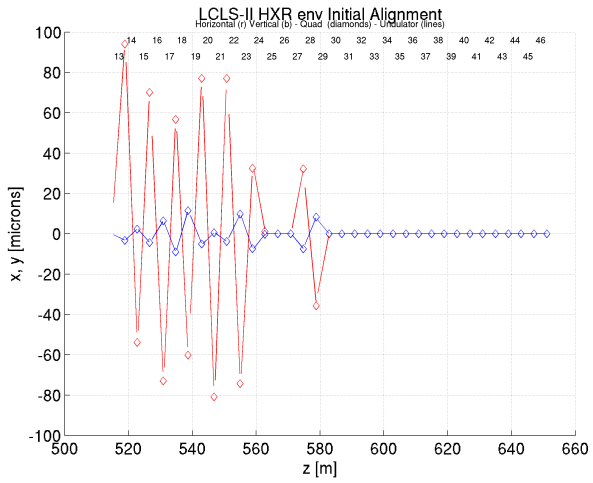

(a) Partial moves based on field integral data.

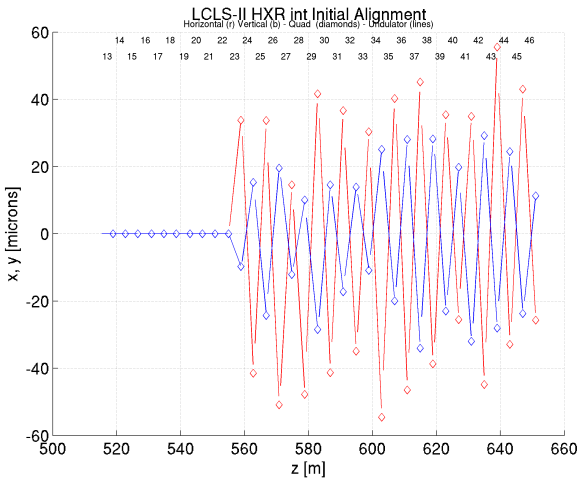

(b) Partial moves based on environmental field data.

Figure 2: Required partial initial moves of the HXR quadruples in horizontal (red) and vertical (blue) directions relative to the cam home positions based environmental (env) and field integral (int) data. The circles indicate the quadrupole positions, the lines indicate the girder center line, illustrating yaw (red) and pitch (blue) angles.

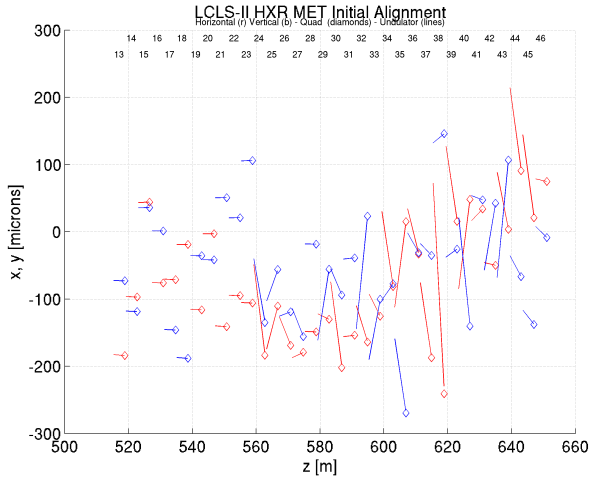

(a) Fractional moves based on metrology mapping data.

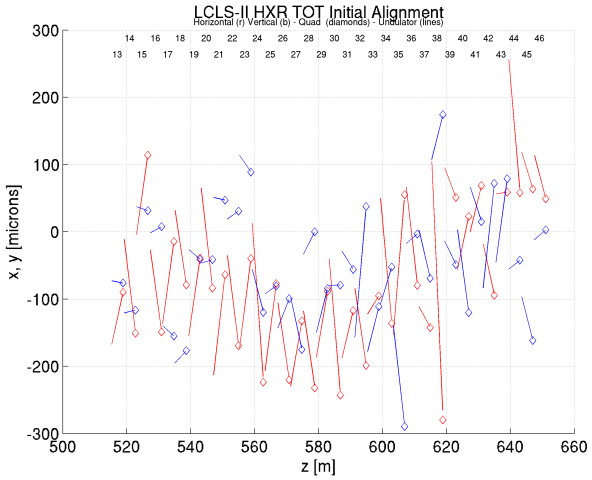

(b) Total Moves.

Figure 3: Required initial moves of the HXR quadruples based on undulator alignment data (MET, partial) and total required moves (TOT, total) including all three contributions. The figure 2 for legend information.

4. SUMMARY

The paper discusses the calculation of the initial cam mover settings for the LCLS-II HXR undulator beamline in preparation for the first beam transport through the system. The final cam angle settings are a function of the girder position mapping data, on-axis environmental field measurements as well as open undulator gap field integrals as results of the undulator segment calibrations.

APPENDIX A. HXR METROLOGY MAPPING RESULT

Table 2: Metrology mapping result: HXR quadrupole center deviations from straight line.

Cell	Z	DX	DY	Yaw	Pitch
	[m]	[mm]	[mm]	[mrad]	[mrad]
13	518.8673	+0.184	+0.073	+0.00035	+0.00014
14	522.7380	+0.097	+0.119	+0.00019	+0.00023
15	526.6076	−0.044	−0.036	−0.00008	−0.00007
16	530.9055	+0.076	−0.001	+0.00014	+0.00000
17	534.7768	+0.071	+0.146	+0.00013	+0.00027
18	538.6455	+0.019	+0.188	+0.00004	+0.00035
19	542.9441	+0.116	+0.036	+0.00021	+0.00007
20	546.8135	+0.003	+0.042	+0.00001	+0.00008
21	550.7546	+0.141	−0.051	+0.00026	−0.00009
22	554.9806	+0.095	−0.021	+0.00017	−0.00004
23	558.8508	+0.106	−0.106	+0.00019	−0.00019
24	562.7915	+0.189	+0.139	+0.03823	+0.02682
25	566.8042	+0.113	+0.058	−0.01803	−0.01314
26	570.8171	+0.169	+0.119	+0.01202	−0.00176
27	574.8296	+0.179	+0.157	−0.00219	+0.01180
28	578.8408	+0.149	+0.018	+0.00026	+0.00003
29	582.8552	+0.130	+0.056	+0.00219	−0.02987
30	586.8677	+0.207	+0.095	+0.03605	+0.01100
31	590.8806	+0.154	+0.039	−0.00055	−0.00053
32	594.8932	+0.164	−0.023	+0.01530	−0.04761
33	598.9057	+0.127	+0.097	+0.00929	−0.02532
34	602.9182	+0.077	+0.078	+0.03169	−0.00679
35	606.9311	−0.015	+0.270	−0.03605	+0.03133
36	610.9436	+0.036	+0.032	+0.01912	+0.00832
37	614.9567	+0.183	+0.034	+0.03168	+0.00495
38	618.9694	+0.241	−0.146	+0.08883	−0.00385
39	622.9820	−0.011	+0.025	+0.03168	−0.00342
40	626.9946	−0.043	+0.134	−0.03769	+0.04565
41	631.0074	−0.034	−0.047	−0.00492	+0.00188
42	635.0199	+0.050	−0.047	+0.00109	−0.02822
43	639.0327	−0.007	−0.100	+0.02404	−0.04956
44	643.0448	−0.091	+0.067	+0.03496	+0.00878
45	647.0578	−0.016	+0.139	+0.03496	+0.00595
46	651.0704	−0.075	+0.008	+0.00109	+0.00474

The metrology group uses a yaw convention different from what is used in this document, which results in oppsite signs for the yaw column. In the former definition, a positive pitch is a rotation around the X axis with the positive Y axis going toward the positive Z axis, the latter is $\psi = \arctan(DX/DZ)$. The numbers in the yaw column in table 2 have been adjusted to conform with the latter convention.

APPENDIX B. HXR ON-AXIS ENVIRONMENTAL FIELD MEASUREMENT RESULT

Table 3 shows the first 3 data rows of file "tunnelfluxplt.run1" as measured by Scott Anderson on August 21, 2019 in the LCLS UH. In the table, slot 11 is equivalent to cell 23. The data is stored in file

`V:\MET\MagServe\MagData\LCLS-II\Background_Fields\HXR_Line\tunnelfluxdat.ru1`

Table 3: Metrology HXR in-tunnel environmental magnetic field measurement result.

slot	xpos(m)	ypos(m)	zpos(m)	BfluxX(T)	BfluxY(T)	BfluxZ(T)
11	0	1.4	0.9	+0.00001215	−0.00005018	+0.00000686
11	0	1.4	1.7	+0.00001234	−0.00004944	+0.00001055
11	0	1.4	2.5	+0.00001153	−0.00006079	+0.00001265

Table 4: Averaged metrology HXR in-tunnel environmental magnetic field measurement data.

cell	$\langle B_x \rangle$ [T]	$\langle B_y \rangle$ [T]
13	+0.0000018	−0.0000480
14	+0.0000012	−0.0000416
15	+0.0000027	−0.0000463
16	+0.0000038	−0.0000594
17	+0.0000059	−0.0000510
18	+0.0000086	−0.0000408
19	+0.0000088	−0.0000503
20	−0.0000015	−0.0000674
21	+0.0000025	−0.0000616
22	+0.0000033	−0.0000604
23	+0.0000120	−0.0000535
24	+0.0000162	−0.0000334
25	+0.0000128	−0.0000373
26	+0.0000094	−0.0000483
27	+0.0000129	−0.0000537
28	+0.0000116	−0.0000498
29	+0.0000177	−0.0000423
30	+0.0000126	−0.0000445
31	+0.0000109	−0.0000427
32	+0.0000139	−0.0000499
33	+0.0000099	−0.0000515
34	+0.0000149	−0.0000263
35	+0.0000087	−0.0000419
36	+0.0000084	−0.0000555
37	+0.0000068	−0.0000430
38	+0.0000095	−0.0000516
39	+0.0000109	−0.0000529
40	+0.0000099	−0.0000566
41	+0.0000128	−0.0000469
42	+0.0000076	−0.0000571
43	+0.0000190	−0.0000565
44	+0.0000098	−0.0000432
45	+0.0000127	−0.0000440
46	+0.0000100	−0.0000339

The data in columns BfluxX(T) and BfluxY(T) of table 3 averaged over all readings for a given slot have been used to calculate the average field amplitudes as listed in table 4. Since the data in table 3 only covers cells 23—46, the data for cells 13—22 are taken from the 2008 measurements*.

*H.-D. Nuhn, LCLS Memorandum, "Initial Undulator Girder Positioning", December 12, 2008

APPENDIX C. HXR UNDULATOR QUADRUPOLE Z SPACINGS

Table 5 lists the z distances between consecutive undulator line quadrupoles. The second column "ΔZ (MET)" shows the difference based on metrology measurements (see table 2), the third column ''ΔZ (MAD)" shows the differences based on the MAD deck while column 4 shows the differences between columns two and three in mm units.

Table 5: HXR undulator quadrupole z spacings.

Name	ΔZ (MET) [m]	ΔZ (MAD) [m]	diff [mm]
QHXH14—QHXH13	3.8707	3.870000	+0.7
QHXH15—QHXH14	3.8696	3.870000	−0.4
QHXH16—QHXH15	4.2979	4.298000	−0.1
QHXH17—QHXH16	3.8713	3.870000	+1.3
QHXH18—QHXH17	3.8687	3.870000	−1.3
QHXH19—QHXH18	4.2986	4.298000	+0.6
QHXH20—QHXH19	3.8694	3.870000	−0.6
QHXH21—QHXH20	3.9411	3.940137	+1.0
QHXH22—QHXH21	4.2260	4.227863	−1.9
QHXH23—QHXH22	3.8702	3.870000	+0.2
QHXH24—QHXH23	3.9407	3.940137	+0.6
QHXH25—QHXH24	4.0127	4.012667	+0.0
QHXH26—QHXH25	4.0129	4.012667	+0.2
QHXH27—QHXH26	4.0125	4.012667	−0.2
QHXH28—QHXH27	4.0112	4.012667	−1.5
QHXH29—QHXH28	4.0144	4.012667	+1.7
QHXH30—QHXH29	4.0125	4.012667	−0.2
QHXH31—QHXH30	4.0129	4.012667	+0.2
QHXH32—QHXH31	4.0126	4.012667	−0.1
QHXH33—QHXH32	4.0125	4.012667	−0.2
QHXH34—QHXH33	4.0125	4.012667	−0.2
QHXH35—QHXH34	4.0129	4.012667	+0.2
QHXH36—QHXH35	4.0125	4.012667	−0.2
QHXH37—QHXH36	4.0131	4.012667	+0.4
QHXH38—QHXH37	4.0127	4.012667	+0.0
QHXH39—QHXH38	4.0126	4.012667	−0.1
QHXH40—QHXH39	4.0126	4.012667	−0.1
QHXH41—QHXH40	4.0128	4.012667	+0.1
QHXH42—QHXH41	4.0125	4.012667	−0.2
QHXH43—QHXH42	4.0128	4.012667	+0.1
QHXH44—QHXH43	4.0121	4.012667	−0.6
QHXH45—QHXH44	4.0130	4.012667	+0.3
QHXH46—QHXH45	4.0126	4.012667	−0.1

APPENDIX D. HXR UNDULATOR SEGMENT OPEN GAP FIELD INTEGRALS

Table 6 lists the first and second field integrals as obtained in the MMF for the installed HXR undulator segments. The field integrals are calculated from the horizontal B_x and vertical B_y magnetic fields measured with a Hall probe along a line of length $L = 4.0125$ m, coinciding with the virtual beam axis inside the undulator segments such that the center of the line is at the center of the undulator segment. The calculation is done in the following way

- First Horizontal Field Integral, $I1x\,(L)$

$$I1x\,(z) = \int_0^z B_x\,(\tilde{z})\,d\tilde{z}$$

- Second Horizontal Field Integral, $I2x\,(L)$

$$I2x\,(z) = \int_0^z I1x\,(\tilde{z})\,d\tilde{z} = \int_0^z \left(\int_0^{\tilde{z}} B_x\left(\tilde{\tilde{z}}\right) d\tilde{\tilde{z}} \right) d\tilde{z}$$

- First Vertial Field Integral, $I1y\,(L)$

$$I1y\,(z) = \int_0^z B_y\,(\tilde{z})\,d\tilde{z}$$

- Second Vertical Field Integral, $I2y\,(L)$

$$I2y\,(z) = \int_0^z I1y\,(\tilde{z})\,d\tilde{z} = \int_0^z \left(\int_0^{\tilde{z}} B_y\left(\tilde{\tilde{z}}\right) d\tilde{\tilde{z}} \right) d\tilde{z}$$

Table 6: First and second field integrals of the installed HXR undulator segments measured in open gap (100 mm) state at the HXR calibration bench in the MMF.

HXR Cell	S/N	$I1x$ [μTm]	$I2x$ [μTm^2]	$I1y$ [μTm]	$I2y$ [μTm^2]
24	HXU-010	+58	+117	−169	−406
25	HXU-030	+37	+83	−92	−268
26	HXU-002	+102	+212	−145	−274
27	HXU-019	+50	+40	−127	−306
29	HXU-027	+67	+111	−193	−548
30	HXU-008	+88	+183	−125	−276
31	HXU-029	+18	+26	−123	−307
32	HXU-009	+65	+146	−104	−223
33	HXU-028	+33	+52	−88	−228
34	HXU-025	+23	+60	−109	−268
35	HXU-022	+82	+256	−167	−451
36	HXU-003	+79	+166	−134	−266
37	HXU-023	+90	+206	−147	−327
38	HXU-026	+93	+227	−113	−240
39	HXU-005	+90	+195	−139	−251
40	HXU-024	+38	+131	−42	−155
41	HXU-006	+106	+198	−119	−266
42	HXU-007	+80	+157	−110	−208
43	HXU-018	+108	+216	−172	−340
44	HXU-021	+34	+97	−111	−274
45	HXU-004	+115	+253	−126	−225
46	HXU-020	+54	+97	−137	−271